Novel host materials for single-component white organic light-emitting diodes based on 9-naphthylanthracene derivatives†

Lei Wang,[a] Wai-Yeung Wong,[a] Mei-Fang Lin,[a] Wai-Kwok Wong,*[a] Kok-Wai Cheah,[b] Hoi-Lam Tam[b] and Chin H. Chen*[ac]

Received 14th April 2008, Accepted 10th July 2008
First published as an Advance Article on the web 18th August 2008
DOI: 10.1039/b806183a

A series of 9-naphthylanthracene based dimers and trimers were synthesized and characterized. TGA studies reveal that they are all thermally stable with decomposition temperatures well above 500 °C. Upon optical excitation, all of these dimers and trimers show intense blue emission in common organic solvents, accompanied by a new peak at long wavelength in the solid state. They exhibit nanosecond transient lifetimes consisting of two decay components, suggesting the formation of excimers. Single-component light-emitting electroluminescent devices based on these robust materials have been fabricated. The device based on 4,4′-bis(9-(1-naphthyl)anthracen-10-yl)biphenyl exhibits a maximum luminance efficiency of 7.0 cd A^{-1} with CIE coordinates of (0.31, 0.36) and luminance of 1396 cd m^{-2} at 6.9 V. The device based on 1,3,5-tris(9-(1-naphthyl)anthracen-10-yl)benzene exhibits a maximum luminance efficiency of 5.78 cd A^{-1} with CIE coordinates of (0.33, 0. 43) and luminance of 1156 cd m^{-2} at 7.8 V.

Introduction

Since the pioneer work by Tang and VanSlyke on efficient organic light-emitting diodes (OLEDs) based on low-molecular-weight compounds,[1] significant progress in materials and device science has led to the realization of full-color OLEDs with improved efficiencies and lifetimes.[2] White OLEDs are a prime focus of OLED research due to their advantages of high resolution and possibility for large-scale production. Considerable achievements in monochromatic efficiency and performance have led to the development of devices with broadband white light emission,[3] in which the white light from a single emissive layer with the formation of electromers,[4] excimers,[5] exciplexes[6] and aggregates[7] was shown to play an important role.

When two aromatic systems are brought into proximity, the propensity for the formation of excimers which are characterized by broad emissive peaks, long lifetimes, and red-shifted emissions[8] is great. It is well known that the formation of excimers will drastically decrease the photoluminescence (PL) quantum yields of the materials because of the greater number of non-radiative decay pathways for depopulation of the excited state.[9] Generally, it is an unwanted effect that often reduces the luminescent efficiency and decreases the emission color purity. However, the excimer does not always play a negative role in highly luminescent materials, for example, the stable excimer is a main source for single-component white light generation.[10] Hou's group[11] reported single-component white electroluminescence (EL) with a maximum brightness of 1395 cd m^{-2} and a current efficiency of 2.07 cd A^{-1} in which the blue emission originated from an isolated molecule and the orange emission from its excimers. Williams *et al.*[12] reported a white organic light-emitting diode (WOLED) with nearly 100% internal quantum efficiency showing current and power efficiencies of 42.5 cd A^{-1} and 29 lm W^{-1}, respectively, using a phosphorescent complex platinum(II) [2-(4′,6′-difluorophenyl)pyridinato-N,$C^{2'}$)] (2,4-pentanedionato).

While anthracene is a well-known and important fluorescent material following the initial report in 1963 by Pope *et al.*[13] on the EL emission from its crystal at a voltage of 400 V, its derivatives have been extensively studied as a subject of great importance in chemical physics.[14] Recently, anthracene derivatives have been shown to be excellent candidates for use in efficient blue OLEDs with high device stability.[15] In some cases, anthracene can also form excimers.[16,17] Ohta and co-workers[16] have reported methylene-linked anthracene and naphthalene molecules and found the methylene chain to play a significant role in the intermolecular excimer formation dynamics and its electric field dependence. It was not until recently that the excimers of aryl-linked dimers and trimers for anthracene derivatives became known and there was a recent preliminary report by us on such a phenomenon based on BUBH-3.[18] Here, we report a detailed study on the synthesis and photophysics of a series of 9-naphthylanthracene based compounds as a new class of host luminescent materials with interesting and potentially useful electroluminescent properties. In a single-component-emitting EL device, some of them can be made to emit white light with

[a]*Centre for Advanced Luminescence Materials, Department of Chemistry, Hong Kong Baptist University, Waterloo Road, Hong Kong, P. R. China*
[b]*Centre for Advanced Luminescence Materials, Department of Physics, Hong Kong Baptist University, Waterloo Road, Hong Kong, P. R. China*
[c]*Display Institute, Microelectronics and Information Systems Research Center, National Chiao Tung University, Hsinchu, Taiwan, 300, Republic of China*

† Electronic supplementary information (ESI) available: Definitions; experimental data. CCDC reference numbers 685067. For ESI and crystallographic data in CIF or other electronic format see DOI: 10.1039/b806183a

high device efficiency, therefore they hold great promise in the fabrication of WOLEDs with simple architectures.

Results and discussion

Synthesis and characterization

The syntheses of compounds **4a–4d** are outlined in Scheme 1. A series of anthracene derivatives were synthesized by the Pd-catalyzed Suzuki cross-coupling of the boronic acid of 9-naphthylanthracene and the corresponding aryl bromide. 9-Naphthylanthracene-10-boronic acid was synthesized by means of lithium bromide exchange at low temperature followed by reaction with tris(isopropyl)borate and subsequent acid hydrolysis. In the patent,[19] Saitoh *et al.* have reported the synthesis of compound **4c** using a divergent methodology, which made the isolation of the final product in high purity very complicated and difficult. Also, the authors did not provided any useful characterization, PL or EL data. To simplify the synthesis, we chose to adopt in this paper a convergent methodology as shown in Scheme 1 in which 9-naphthylanthracene-10-boronic acid was first synthesized as the common synthon. It was then reacted with the corresponding aryl bromide to give the product which, owing to its poor solubility, precipitated directly from the reaction mixture, and thus could be obtained in high yield by simple filtration. Further purification was readily accomplished by train sublimation in vacuum (10^{-6} Torr). Some of these compounds (like **4b**) are too insoluble in most common organic solvents even at 60 °C to collect the NMR spectra.

Crystal structure

In order to look at the conformation of these anthracene derivatives, the crystal structure of **4c** was determined. As shown in Fig. 1 (left), the molecules of **4c** were found to possess a propeller twist topology in the crystal, and the dihedral angles between the central phenyl core and the coordinated anthracene rings are 83.7(1), 61.8(1) and 67.1(1)° while the dihedral angles between the 1-naphthyl and anthracene planes are 87.7(1), 68.6(1) and 85.2(1)°. According to its crystal packing, it is clear that the molecules tend not to aggregate in the ground state. With the additional steric hindrance of the 1-naphthyl ring, it is only possible for the molecules to react with each other by edge-to-edge interaction.

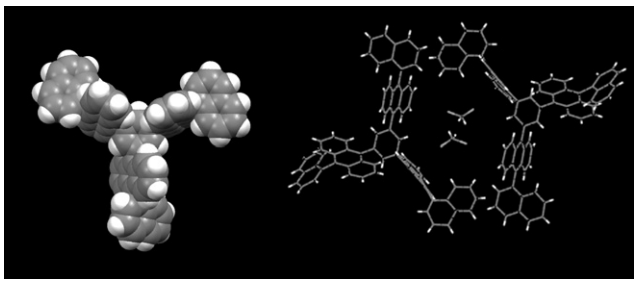

Fig. 1 A perspective view of the space-filling model of compound **4c** and its crystal packing showing two formula units related by an inversion centre at (0.5, 0.5, 0.5). The dichloromethane solvates shown have 0.5 occupancy.

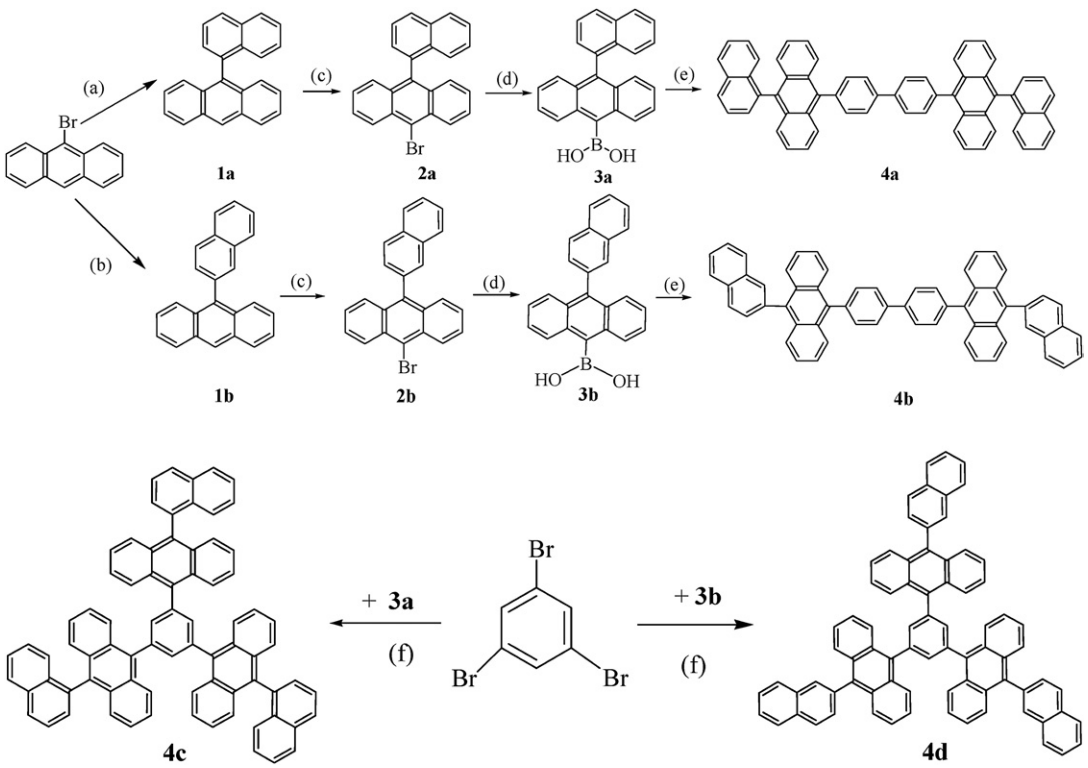

Scheme 1 Synthesis of compounds **4a**, **4b**, **4c** and **4d**. *Conditions*: (a) $PdCl_2(PPh_3)_2$, toluene, 2 M K_2CO_3, 1-naphthyl boronic acid; (b) $PdCl_2(PPh_3)_2$, toluene, 2 M K_2CO_3, 2-naphthyl boronic acid; (c) *hν*, NBS, CH_2Cl_2; (d) n-BuLi, toluene–ether; tris(isopropyl) borate, HCl; (e) 4,4′-diiodobiphenyl, $Pd(PPh_3)_4$, THF, 2 M K_2CO_3; (f) $Pd(PPh_3)_4$, toluene–EtOH, 2 M Na_2CO_3.

Table 1 The optical, photophysical and thermal properties of **4a**, **4b**, **4c** and **4d**

	4a	4b	4c	4d
PL film λ/nm	444, 547	457, 513, 544	440, 540	456, 498, 538
PL solution $\lambda_{a,\ max}$/nm[a]	416, 434	430	414, 432	422, 440
Φ_f [b]	0.58	0.50	0.68	0.59
Abs film λ/nm	361, 381, 402	364, 384, 405	361, 382, 404	362, 383, 405
Abs solution/ $\lambda_{a,max}$/nm[a]	358, 376, 397	359, 378, 398	359, 378, 399	359, 379, 401
$E_{1/2}^{ox}$/eV	1.27	1.25	1.31	1.29
HOMO	−5.57	−5.55	−5.61	−5.59
LUMO/eV	−2.59	−2.58	−2.61	−2.60
Band gap/eV	2.98	2.97	3.00	2.99
T_d/°C	510	535	542	539

[a] The absorption and PL spectra in CH_2Cl_2. [b] PL quantum yield relative to quinine sulfate in 1 N H_2SO_4.

Thermal and electrochemical behavior

The thermal properties of these new compounds were determined by DSC and TGA measurements and the thermal stability data are listed in Table 1. They all possess very high thermal stabilities with decomposition temperatures well above 500 °C, but exhibit no discernible glass transition temperatures (T_g). Their evaporated films exhibit only a broad halo in the X-ray diffraction patterns (see ESI†) which indicates that they form uniform amorphous films by vacuum deposition. All of the newly synthesized compounds were characterized by cyclic voltammetry and the data are listed in Table 1. In each case, the anodic scan was performed in CH_2Cl_2. A reversible oxidation wave was observed at half-wave potentials ($E_{1/2}$) of 1.25–1.31 V. With the same core, the compounds containing a 2-naphthyl group have lower E^{ox} and smaller energy gaps than the compounds containing 1-naphthyl groups, which might be attributed to the stronger donor ability of the 2-naphthyl group. The HOMO/LUMO levels of these compounds, which were calculated from the E^{ox} and the optical band gap (estimated from the absorption edge), are listed in Table 1.

Photophysical properties

Absorption and PL spectra of compounds **4a–4d** in dilute dichloromethane solution and film substrate on quartz are shown in Fig. 2. On irradiation at 376 nm in CH_2Cl_2, all of the compounds show intense blue fluorescence, with an emission peak centered at 417–430 nm. The PL quantum yields (Φ_f) of these compounds are listed in Table 1.The absorption bands are centered within the region of 330–400 nm, and they are assigned to the $S_1 \leftarrow S_0$ transition of the anthracene moiety.[16,19] The position of the 0–0 transition to the S_1 state remains almost unchanged with changes in the aryl core and peripheral chromophores. In solution, there is a slight red shift in the

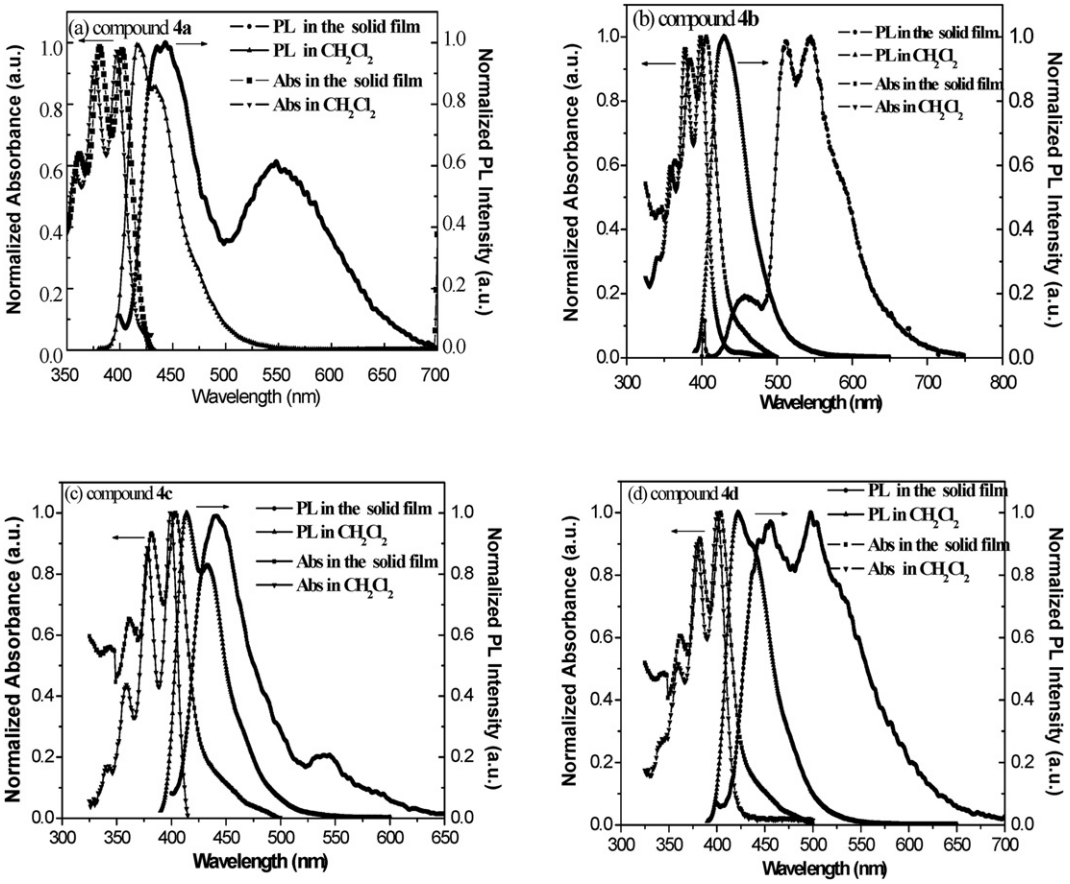

Fig. 2 Photoluminescence (PL) (λ_{ex} = 376 nm) and absorption spectra of compounds **4a**, **4b**, **4c** and **4d** in dichloromethane solution and as solid films.

absorption and PL maxima of **4b** and **4d** as compared to **4a** and **4c**, respectively, and this is likely due to a decrease in conjugation because of the higher steric hindrance of the 1-naphthyl compared to the 2-naphthyl moiety. Meanwhile, the trimer has a slight blue shift as compared to the corresponding dimer, which may be attributed to π-system distortion because of the propeller twist topology of the trimer.[20]

The absorption and PL spectra of thin films of **4a–4d** are also shown in Fig. 2. The solid-state emission bands of the dimers and trimers are very broad and an additional broad emission at 500–570 nm tailing to 650 nm is also observed in each case. Compared to the solution PL spectra, the typical peak of anthracene is red-shifted by 25–35 nm (Table 1). These features are usually observed for organic and polymer materials presumably due to intermolecular interactions or exciton hopping in the solid state,[21] but the appearance of the orange emission is very interesting, which suggests the formation of a new species in the solid film.

In both the solution phase and solid thin film, all of the compounds have similarly structured absorption spectra in the 330–440 nm region. The broad orange emission at around 540 nm may be ascribed to the excimer formation due to the naphthyl-to-naphthyl interactions based on the edge-to-edge model revealed in the X-ray crystallographic analysis. To further explore the photophysics of these new 9-naphthylanthracene derivatives, we obtained PL decay dynamics information. The PL decay dynamics of **4a–4d** are exemplified by the PL decay curves and the data are shown in Table 2. All of these compounds in the solid films are rather long-lived in the excited state with the dominant fluorescence lifetimes in the range of 0.28–2.36 ns. Meanwhile, the radiative lifetimes increase as the spectrally selected band shifts toward the long wavelength emission threshold, which suggest the formation of at least one more well-defined excimer. These PL decay dynamics results are also in accordance with the interpretation of the steady-state emission in thin films due to intermolecular excimers.[22] We also note that the nanosecond scale of the decay times could rule out the involvement of possible triplet excitons and their excimers as a possible source of the long-wavelength emission band.[23] As a result, it is reasonable to assign the additional broad orange emission band to singlet excimeric states formed by anthracene derivatives in the solid state.

As shown in Fig. 2, in the solid-state PL spectra of the dimers or trimers, compounds containing a 2-naphthyl group show stronger peaks in the long-wavelength regime than those with the 1-naphthyl moiety. This suggests the peripheral aryl group plays an important role in the formation of excimers, and the 2-naphthyl ring has a smaller steric hindrance than the 1-naphthyl counterpart and thus is more prone to form the excimer.

Table 2 Excited state lifetimes (in ns) of **4a**, **4b**, **4c** and **4d** in thin film at different wavelengths

Compound	430 nm	460 nm	490 nm	530 nm	550 nm
4a	0.35	0.36	0.38	1.36	2.36
4b	0.34	0.47	0.53	1.02	2.21
4c	0.31	0.45	0.49	1.13	1.61
4d	0.28	0.38	0.42	0.90	1.52

Meanwhile, the long wavelength peak of **4c** is weaker than that of **4a** and it can be explained by the propeller twist topology structure of **4c**, which makes the formation of excimers more difficult.

Electroluminescence properties

We explored the performance characteristics of the devices using these compounds as the light-emitting layer in single-layer and triple-layer devices (see Scheme 2). Fig. 3b and Fig. 3d show the EL spectra of **4b a**nd **4d** in devices **I** and **II**. Compared to their PL spectra, the EL spectra were almost unchanged except for a slight red shift of the emission maximum. But the EL spectra of **4a** and **4c** show an obvious change in shape compared to their PL spectra with the blue peak decreased and the orange peak increased in intensity, even though their peak position does not change much. This suggests that the EL emission selectively occurs at the excimer sites.[24] Since compounds **4a** and **4c** contain 1-naphthyl units which have high steric hindrance, their excimers are not as stable as those of **4b** and **4d**. When the current density reaches a threshold level, electroluminescence is likely to occur from the emissive site of the excimers. If the current density is near or beyond the threshold, the emission at the excimer will become weaker. As shown in Fig. 3a and 3c, the blue peak plays a more important role in the EL spectra of **4a** and **4c** as the current density increases from 20 to 200 mA cm^{-2}. Comparing the EL spectra of the single-layer device and the three-layer device of all compounds, no new peaks were observed, and the overall EL pattern of triple-layer device **II** is similar to that of the single-layer device **I**, which suggest the long-wavelength EL emissions of these devices should have similar origins (*i.e.* excimer). This result also rules out the possibility of formation of a species such as an exciplex at the NPB/Host interface (or Alq_3/Host interface) in device **II**.

The current efficiency *versus* current density and the current density–voltage characteristics of these compounds in the triple-layer devices (device **II**) are shown in Fig. 4, and the EL data of the four OLEDs are listed in Table 3. In device **II** for compound **4a**, the emission is close to white with Commission Internationate de'Eclairage ($CIE_{x,y}$) coordinates of (0.31, 0.36) to (0.29, 0.32) when the drive current increased from 20 to 200 mA cm^{-2} (Fig. 3), which shows a maximum efficiency of 7.0 cd A^{-1} and a brightness of 1396 cd m^{-2} at 20 mA cm^{-2}. Compound **4c** also emits white light with $CIE_{x,y}$ of (0.33, 0.43) and a maximum efficiency of 5.78 cd A^{-1} and brightness of 1156 cd m^{-2} at 20 mA cm^{-2}. In contrast, compounds **4b** and **4d** emit green-yellow and

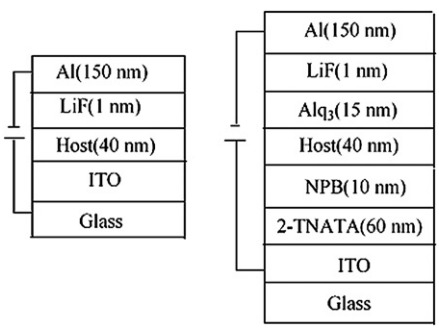

Scheme 2 The structures of devices **I** and **II**.

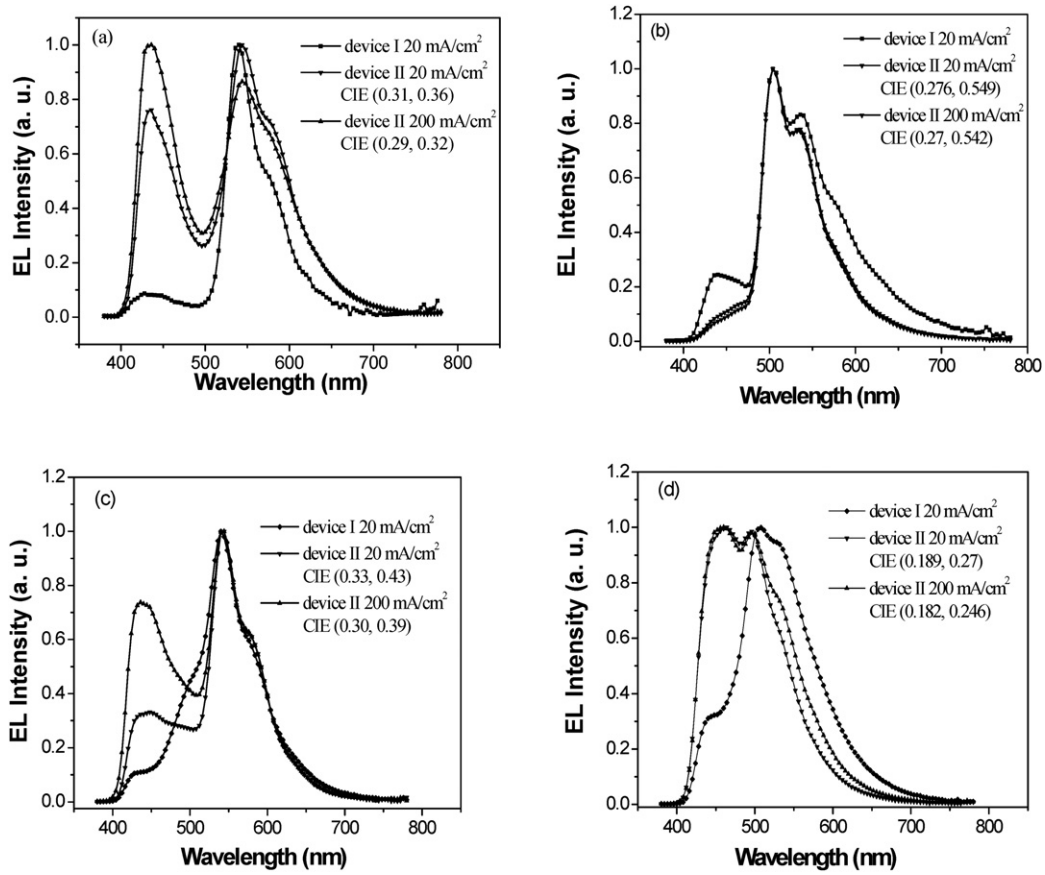

Fig. 3 Electroluminescence (EL) spectra of (a) **4a**, (b) **4b**, (c) **4c** and (d) **4d** based devices **I** and **II**.

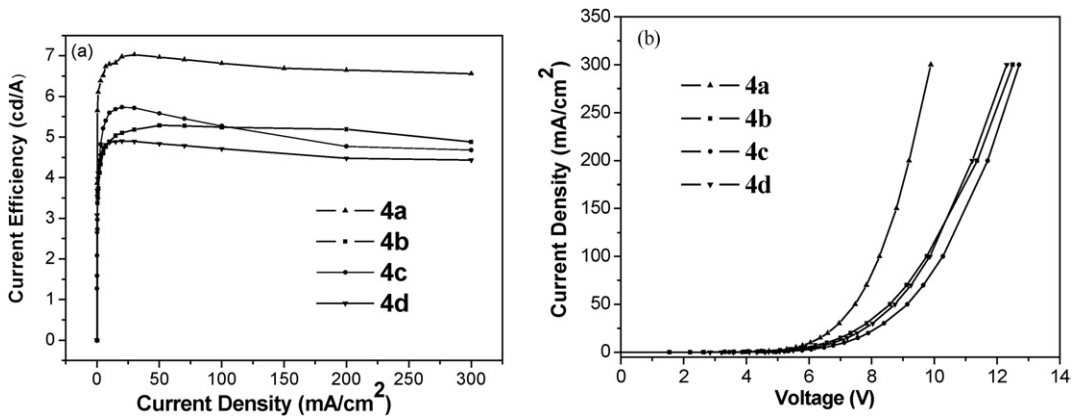

Fig. 4 (a) Dependence of the current efficiency on the drive current density for **4a–4d** based devices **II**.(b) Current density–voltage (*J*–*V*) curves.

Table 3 The EL performance of **4a–4d** in the triple-layer device **II**

	Current/ mA cm^{-2}	Brightness/ cd m^{-2}, V	Current efficiency/ cd A^{-1}	Power efficiency/ lm W^{-1}	EQE (%)	CIE$_{x,y}$
4a	20	1396, 6.9	7.0	3.2	2.71	(0.31,0.36)
4b	20	1020, 7.3	5.1	2.04	1.67	(0.28,0.55)
4c	20	1156, 7.8	5.78	2.30	1.96	(0.33,0.43)
4d	20	980, 7.4	4.9	2.07	1.97	(0.19,0.27)

green-blue light respectively, and their color only changes slightly with the current density because their excimers are more stable (Fig. 3). In summary, the 9-naphthylanthracene based trimers and dimers can form excimers in the solid state, and the peripheral groups of anthracene control the stability of the excimer and its associated long-wavelength emission. With the judicious choice of peripheral group and core, these new luminescent materials can be fabricated to emit white light with high current efficiency in a simple device structure.

Conclusions

A series of new luminescent materials based on 9-naphthylanthracene have been prepared *via* a high-yield convergent synthesis and characterized. All of them possess good thermal stabilities with no detectable glass transitions. They emit deep blue emission in solution, but a new peak at longer wavelength appeared in the solid films. Detailed study of their photophysics shows that the latter peak has nanosecond lifetime with two components in the neat films. The presence of the delayed component is attributed to the formation of excimers. We find the peripheral steric bulky group plays an important role in controlling the stability of the excimer and its associated long-wavelength emission. Single-emitting-component EL devices of theses compound were fabricated. When compounds **4a** and **4c** were used as hosts, they exhibited bright and efficient white light with good luminance and high current efficiency at a low drive voltage. Since WOLEDs with a single-emitting-component may greatly simplify the fabrication process, the small molecular luminescent materials described in this report are promising for future WOLED displays and lighting applications. Further investigations along this line are currently continuing in our laboratory.

Experimental

Material and methods

1-Naphthyl boronic acid, 2-naphthyl boronic acid and 9-bromoanthracene were used as received from Aldrich. The solvents were used as supplied or purified by the standard techniques. All reactions requiring anhydrous condition were performed in oven-dried glassware under a N_2 atmosphere using Schlenk flask techniques. The experimental data of the known compounds of **1a**, **1b**, **2a**, **2b** are given in the ESI.† ^{1}H and ^{13}C NMR spectra were recorded on a JEOLEX 270 spectrometer or a Bruker-AF301 AT 400 MHz spectrometer. The infrared spectra were measured on a Nicolet 670 FT-IR spectrophotometer. Low-resolution mass spectra were obtained on a Finnigan MAT SSQ-710 in FAB (positive) mode. High resolution mass spectrometric measurements were carried out using a Bruker autoflex MALDI-TOF mass spectrometer. Fluorescence spectra were obtained on a Perkin Elmer LS55 Luminescence spectrometer. The differential scanning calorimetry (DSC) analysis was performed under a nitrogen atmosphere on a TA Instruments DSC 2920. Elemental analyses were determined by a Finnigan FLASH 1112 SERIES EA elemental autoanalyzer. To measure the PL quantum yields (Φ_f), degassed solutions of the compounds in CH_2Cl_2 were prepared. The concentration was adjusted so that the absorbance of the solution would be lower than 0.1. The excitation was performed at the 360 nm, and a solution in 1 N H_2SO_4 of quinine sulfate, which has $\Phi_f = 0.546$, was used as a standard.[24] Cyclic voltammetric measurements were carried out in a conventional three electrode cell using a Pt button working electrode of 2 mm in diameter, a platinum wire counter electrode, and a SCE reference electrode on a computer-controlled EG&G Potentiostat/Galvanostat model 283 at room temperature. Reduction CV of all compounds was performed in dichloromethane containing Bu_4NPF_6 (0.1 M) as the supporting electrolyte.

Device fabrication

Prior to the deposition of organic materials, the indium-tin-oxide (ITO)/glass was cleaned with a routine cleaning procedure and pretreated with UV-ozone. Devices were fabricated under a base vacuum of about 10^{-6} Torr in a thin-film evaporation coater following a published protocol.[25] In the device, 2-TNATA (4,4′,4″-tris-*N*-napthyl-*N*-phenylamino-triphenylamine) was used as the hole-injection layer, NPB (*N*,*N*″-bis(1-naphthyl)-*N*,*N*′-diphenyl-1,1,1′-biphenyl-4,4′-diamine) served as hole-transporting layer, and tris(8-hydroxyquinoline)aluminium (Alq_3) was used as the electron-transporting layer. The current–voltage–luminance characteristics of the devices were measured with a diode array rapid scan system using a Photo Research PR650 spectrophotometer and a computer-controlled, programmable, direct-current (DC) source.

Single-crystal structure analysis

Diffraction data were collected at 293 K using graphite monochromated Mo-Kα radiation ($\lambda = 0.71073$ Å) on a Bruker Axs SMART 1000 CCD diffractometer. The collected frames were processed with the software SAINT+[26] and an absorption correction (SADABS)[27] was applied to the collected reflections. The structure was solved by direct methods (SHELXTL)[28] in conjunction with standard difference Fourier techniques and subsequently refined by full-matrix least-squares analyses on F^2. Crystallographic data for **4c**: $C_{78}H_{48}\cdot 0.5CH_2Cl_2$, $M_r = 1027.63$, crystal dimensions $0.32 \times 0.25 \times 0.23$ mm^3, triclinic, space group $P\bar{1}$, $Z = 2$, $a = 15.349(1)$ Å, $b = 15.706(1)$ Å, $c = 15.789(1)$ Å, $\alpha = 66.033(1)^\circ$, $\beta = 61.608(1)^\circ$, $\gamma = 62.436(1)^\circ$, $U = 2882.6(3)$ Å^3, $\rho_{calcd} = 1.184$ g cm^{-3}, $F(000) = 1074$. A total of 13788 reflections were measured in the range $2.54 \le \theta \le 25.00$ (*hkl* indices: $-17 \le h \le 18$, $-13 \le k \le 18$, $-18 \le l \le 18$), 9623 unique reflections. The structure was refined on F^2 to $wR2 = 0.2973$, $R1 = 0.1315$ (6089 reflections with $I > 2\sigma(I)$, GOF = 0.979 on F^2 for 725 refined parameters).†

Synthesis

9-(1-Naphthyl)anthracene-10-boronic acid (3a). To a slurry containing (11.52 g, 30 mM) dry 9-(1-naphthyl)-10-bromoanthracene in 250 mL of dry toluene and 250 mL of dry diethyl ether under nitrogen atmosphere in a 1 L three-necked round flask cooled in a dry ice-acetone bath was added dropwise 16 mL of 2.5 M *n*-butylithium solution in hexane with stirring within a period of 30 min. Stirring was continued for another 2 h. Tri(isopropyl)borate (40 mM, 1.3 eq) was added over 20 min, then the mixture was equilibrated to room temperature and stirred for an additional 12 h. The mixture was then cooled in a dry ice bath and 100 mL of 2 M HCl and 50 mL of toluene were added . The organic layer was washed with water and dried with Na_2SO_4, filtered and hexane was added to the concentrated organic layer from which a lot of white solid was precipitated. The solid was dissolved in 100 mL of THF and 10 mL of concentrated HCl and 100 mg of *tetra*(n-butyl)ammmonium bromide were added. The mixture was stirred overnight at r.t. and the voluminous solid precipitate was isolated by filtration to give 7.6 g of the product as a white solid. Yield 75%. ^{1}H NMR (400 MHz, $CDCl_3$): δ 8.96 (s, 2H), 8.17 (d, 1H, $J = 4.4$Hz), 7.09–

8.16 (m, 3H), 7.75–7.77 (m, 1H), 7.47–7.50 (m, 4H), 7.22–7.31 (m, 5H). 6.84–6.86 (m, 1H); IR (KBr, cm^{-1}): 3052 (s), 2870, 1559 (s), 1509 (s), 1411 (s), 1313 (s), 1254 (s), 1107 (s), 1047 (s), 949 (s), 761 (s), 655(s); MALDI-TOF-MS *m/z* calcd for $C_{24}H_{17}BO_2$ $[M]^+$, 348.1320; found, 348.1308.

9-(2-Naphthyl)anthracene-10-boronic acid (3b). ^1H NMR: (400 MHz, $CDCl_3$): 8.17 (d, 2H, $J = 8.8$ Hz), 8.0–8.06 (m, 2H), 7.89–7.91 (m, 2H), 7.68–7.90 (m, 2H),7.58–7.60 (m, 2H), 7.47–7.53 (m, 3H). 7.3–7.34 (m, 2H). IR (KBr, cm^{-1}): 3052 (s), 2975(s), 2877(s), 1599 (s), 1559 (s), 1411 (s), 1316 (s), 1263 (s), 1127 (s), 1046 (s), 946 (s), 821(s), 757 (s), 653 (s). MALDI-TOF-MS *m/z* calcd for $C_{24}H_{17}BO_2$ $[M]^+$, 348.1320; found, 348.1306.

4,4′-Bis(9-(1-naphthyl)anthracen-10-yl)biphenyl (4a). A mixture of 9-(1-naphthyl)anthracene-10-boronic acid (9.72 g, 30 mmol), tetrakis(triphenylphosphine)palladium(0) (405 mg, 0.3 mmol), 4,4′-di(iodo)biphenyl (6.08 g, 15 mmol), tetrahydrofuran (300 mL), and 2 M K_2CO_3 (100 mL) were heated at 80 °C with magnetic stirring under nitrogen atmosphere. Some solid began to appear after 2 h and heating was continued overnight. The reaction mixture was cooled to room temperature and the precipitated solid was isolated by filtration, washed with water, then air dried to yield 9.72 g (85%) of the product. ^1H NMR (270 MHz, $CDCl_3$, 50 °C): δ 7.18–7.27 (8H, m), 7.34–7.40 (4H), 7.46–7.51 (m, 6H), 7.59–7.61 (m, 2H), 7.69–7.76 (m, 6H), 7.87–7.91 (m, 4H), 8.0–8.09 (m, 8H). IR (KBr, cm^{-1}): 3035 (s), 1586 (s), 1502 (s), 1437 (s), 1372 (s), 1010 (s), 934 (s), 769 (s), 699 (s); MALDI-TOF-MS *m/z* calcd for $C_{60}H_{38}$ $[M]^+$, 758.2968; found, 758.2974. Anal. calcd for $C_{60}H_{38}$: C, 94.95; H, 5.05; Found: C, 94.85; H, 5.15%.

4,4′-Bis(9-(2-naphthyl)anthracen-10-yl)biphenyl (4b). The compound was synthesized in a similar way as **4c**. Its solubility is very poor. IR (KBr, cm^{-1}): 3038 (s), 1627(s), 1598(s), 1586 (s), 1499 (s), 1439 (s), 1393 (s), 1372 (s), 1028 (s), 934 (s), 769 (s); MALDI-TOF-MS *m/z* calcd for $C_{60}H_{38}$ $[M + 1]^+$, 759.3046; found, 759.3043. Anal. calcd for $C_{60}H_{38}$: C, 94.95; H, 5.05; Found: C, 94.83; H, 5.17%.

1,3,5-Tris(9-(1-naphthyl)anthracen-10-yl)benzene (4c). A mixture of 9-(1-naphthyl)anthracene-10-boronic acid (4.5 g, 13 mmol), tetrakis(triphenylphosphine)palladium(0) (405 mg, 0.3 mmol), 1,3,5-tribromobenzene (0.91 g, 2.89 mmol), toluene (200 mL), ethanol (100 mL) and 2 M K_2CO_3 (150 mL) were heated at 100 °C for 12 h with magnetic stirring under nitrogen atmosphere. The reaction mixture was cooled to room temperature and the precipitated solid was isolated by filtration, washed with water, then recrystallized from dichloromethane–n-hexane to yield 2.5 g (87%) of the product. The yield is calculated according to aryl bromide. ^1H NMR (400 MHz, $CDCl_3$) δ 8.35 (d, $J = 8.8$ Hz, 6H), 7.98–8.05 (m, 9H), 7.67–7.7 (m, 3H), 7.52–7.57 (m, 9H), 7.43–7.47 (m, 9H),7.25–7.29 (m, 6H), 7.09–7.19 (m, 6H); ^{13}C NMR ($CDCl_3$) δ 139.57, 136.91, 135.67, 134.46, 134.31, 134.22, 133.91, 133.81, 130.99, 130.29, 129.43, 128.44, 128.38, 127.54, 127.11, 126.83, 126.54, 126.24, 125.83, 125.51; IR (KBr, cm^{-1}): 3058 (s), 1586 (s), 1506 (s), 1439 (s), 1363 (s), 1028 (s), 915 (s), 798 (s), 778 (s), 764 (s), 726 (s); MALDI-TOF-MS *m/z* calcd for $C_{78}H_{48}$ $[M]^+$, 984.3751, found 984.3761. Anal. calcd for $C_{78}H_{48}$: C, 95.09; H, 4.91; Found: C, 95.02; H, 4.98%.

1,3,5-Tris(9-(2-naphthyl)anthracen-10-yl)benzene (4d). The compound was synthesized using a similar procedure to that for **4c**. Yield 2.28 g (80%). The yield is calculated according to aryl bromide. ^1H NMR (400 MHz, $CDCl_3$) δ 8.31 (d, $J = 8.8$ Hz, 6H), 7.99–8.07 (m, 6H), 7.89–7.96 (m, 9H), 7.72–7.74 (m, 6H), 7.53–7.57 (m, 15H), 7.33–7.37 (m, 6H). ^{13}C NMR ($CDCl_3$) δ 139.53, 137.57, 136.74, 136.69, 134.28, 133.62, 133.0, 130.46, 130.42, 130.25, 129.76, 128.34, 128.22, 128.13, 127.53, 127.06, 126.67, 126.47, 125.77, 125.41; IR (KBr, cm^{-1}): 3054 (s), 1627(s), 1583 (s), 1503 (s), 1437 (s), 1365 (s), 1027 (s), 924 (s), 818, 766(s), 744 (s), 726(s); MALDI-TOF-MS *m/z* calcd for $C_{78}H_{48}$ $[M + 1]^+$, 985.3748, found 985.3752. Anal. calcd for $C_{78}H_{48}$: C, 95.09; H, 4.91; Found: C, 95.01; H, 4.99%.

Acknowledgements

This work is supported by the central allocation grant from the Research Grants Council of Hong Kong SAR (GHP/057/05) and Faculty Research Grant (FRG/05-06/II-43) of HKBU.

References

1 C. W. Tang and S. A. VanSlyke, *Appl. Phys. Lett.*, 1987, **51**, 913.
2 (*a*) Y. Shirota, *J. Mater. Chem.*, 2005, **15**, 75; (*b*) B. W. D'Andrade and S. R. Forrest, *Adv. Mater.*, 2004, **16**, 1585; (*c*) C. T. Chen, *Chem. Mater.*, 2004, **16**, 4389.
3 (*a*) Q. F. Xu, H. M. Duong, F. Wud and Y. Yang, *Appl. Phys. Lett.*, 2004, **85**, 3357; (*b*) H. A. Al Attar, A. P. Monkman, M. Tavasli, S. Bettington and M. R. Bryce, *Appl. Phys. Lett.*, 2005, **86**, 121101.
4 X. J. Xu, G. Yu, C. A. Di, Y. Q. Liu, K. F. Shao, L. M. Yang and P. Lu, *Appl. Phys. Lett.*, 2006, **89**, 123503.
5 S. Y. Chen, X. J. Xu, Y. Q. Liu, W. F. Qiu, G. Yu, H. P. Wang and D. B. Zhu, *J. Phys. Chem. C*, 2007, **111**, 1029.
6 P. K. Abhishek and A. J. Samson, *J. Phys. Chem. C*, 2008, **112**, 5174.
7 J. Kalinowski, G. Giro, M. Cocchi, V. Fattori and P. Di Marco, *Appl. Phys. Lett.*, 2000, **76**, 2352.
8 (*a*) M. Sims, D. D. C. Bradley, M. Ariu, M. Koeberg, A. Asimakis, M. Grell and D. G. Lidzey, *Adv. Funct. Mater.*, 2004, **14**, 765.
9 A. P. Kulkarni, X. Kong and S. A. Jenekhe, *J. Phys. Chem. B*, 2004, **108**, 8689.
10 Y. Kim, J. Bouffard, S. E. Kooi and T. M. Swager, *J. Am. Chem. Soc.*, 2005, **127**, 13726.
11 Y. Liu, M. Nishiura, Y. Wang and Z. M. Hou, *J. Am. Chem. Soc.*, 2006, **128**, 5592.
12 E. L. Williams, K. Haavisto, J. Li and G. E. Jabbour, *Adv. Mater.*, 2007, **19**, 197.
13 M. Pope, H. P. Kallmann and P. Magnante, *J. Chem. Phys.*, 1963, **38**, 2042.
14 (*a*) G. Q. Zhang, G. Q. Yang, S. Q. Wang, Q. Q. Chen and J. S. Ma, *Chem.–Eur. J.*, 2007, **13**, 3630; (*b*) D. R. Cao, S. Dobis and H. Meier, *Tetrahedron Lett.*, 2002, **43**, 6853.
15 (*a*) M. S. Kim, B. K. Choi, T. W. Lee, D. W. Shin, S. K. Kang, J. M. Kim, S. Tamura and T. Y. Noh, *Appl. Phys. Lett.*, 2007, **91**(25), 251111; (*b*) M. H. Ho, Y. S. Wu, S. W. Wen, M. T. Lee, T. M. Chen, C. H. Chen, K. C. Kwok, S. K. So, K. T. Yeung, Y. K. Cheng and Z. Q. Gao, *Appl. Phys. Lett.*, 2006, **89**(25), 252903; (*c*) Z. Q. Gao, B. X. Mi, C. H. Chen, K. W. Cheah, Y. K. Cheng and W. S. Wen, *Appl. Phys. Lett.*, 2007, **90**(12), 123506.
16 T. Nakabayashi, B. Wu, T. Morikaw, T. Iimori, M. B. Rubin, S. Speiser and N. Ohta, *J. Photochem. Photobiol., A: Chem.*, 2006, **178**, 236.
17 X. Wang, D. H. Levy, M. B. Rubin and S. Speiser, *J. Phys. Chem. A*, 2000, **104**, 6558.
18 L. Wang, M. F. Lin, W. K. Wong, H. L. Tam, K. W. Cheah and C. H. Chen, *Appl. Phys. Lett.*, 2007, **91**, 183504.

19 A. Saitoh, S. Akihiro, K. Ueno, K. J. Okinaka and K. Suzuki, *Eur. Pat. Appl.*, 2004, EP 1491610 A2 20041229.
20 H. P. Rathnayake, A. Cirpan, F. E. Karasz, M. Y. Odoi, N. I. Hammer, M. D. Barnes and P. Lahti, *Chem. Mater.*, 2004, **19**, 3265.
21 (*a*) J. Y. Li, D. Liu, C. Ma, O. Lengyel, C. S. Lee, C. H. Tung and S. T. Lee, *Adv. Mater.*, 2004, **16**, 1538; (*b*) N. J. Turro, *Modern Molecular Photochemistry*, Benjamin/Cumming Publishing Company, Menlo Park, CA, 1978.
22 (*a*) T. W. Kwon, M. M. Alam and S. A. Jenekhe, *Chem. Mater.*, 2004, **16**, 4657; (*b*) J. A. Osaheni and S. A. Jenekhe, *Macromolecules*, 1994, **27**, 739.
23 J. Kalinowski, G. Giro, M. Cocci, V. Fattori and P. D. Marco, *Appl. Phys. Lett.*, 2000, **76**, 2352.
24 J. A. Mikroyannidis, L. Fenenko and C. Y. Adachi, *J. Phys. Chem. B*, 2006, **110**, 20317.
25 S. A. Van Slyke, C. H. Chen and C. W. Tang, *Appl. Phys. Lett.*, 1996, **69**, 2160.
26 *SAINT+, ver. 6.02a*, Bruker Analytical X-ray System Inc., Madison, WI, 1998.
27 G. M. Sheldrick, *SADABS, Empirical Absorption Correction Program*, University of Göttingen, Germany, 1997.
28 G. M. Sheldrick, *SHELXTL™, Reference Manual, ver. 5.1*, Madison, WI, 1997.

